CrossMark

Causes responsible for intense and severe storms during the declining phase of Solar Cycle 24

KALPANA PATEL[1], ABHA SINGH[2], S. B. SINGH[3] and A. K. SINGH[3,*]

[1]Department of Physics, SRM Institute of Science and Technology, Modinagar 201 204, India.
[2]Department of Physics, T. D. P. G. College, Jaunpur 222 002, India.
[3]Department of Physics, Banaras Hindu University, Varanasi 221 005, India.
*Corresponding author. E-mail: abhay_s@rediffmail.com

Abstract. The occurrence of total 113 geomagnetic storms during declining phase of Solar Cycle 24 (2015–2017) subdivided as about 105 moderate storms (Dst = −50 nT to −100 nT), 6 intense storms (Dst = −100 nT to −200 nT) and 2 severe storms (Dst < −200 nT) has been diagnosed on the basis of 5 day active window through the CACTus (Computer aided CME tracking) software. A detailed study has been carried out for the 6 intense and 2 severe storms. It is inferred that CMEs are the major source of geomagnetic storms to occur. Out of the 6 intense and 2 severe storms, only 1 has been observed with the origin of CIR. Thus, all analyzed intense geomagnetic storms are due to coronal mass ejection at the Sun. Most of our results are in good accordance with other reported results.

Keywords. Geomagnetic storms—coronal mass ejections (CME)—space weather—severe storms.

1. Introduction

Sun is the main source of space weather and ultimate source of energy for the solar system, as it releases energy continuously in the form of electromagnetic radiation, charged particles and magnetic fields which are responsible for the formation and dynamics of the Earth's ionosphere and magnetosphere (Siscoe and Schwenn 2006). A variety of physical phenomena are associated with space weather, including geomagnetic storms, energization of the Van-Allen radiation belts, geomagnetic activity, ionospheric disturbances, scintillations, aurora and geomagnetically induced currents at the Earth's surface (Singh *et al.* 2010). The inaccurate interpretation of these space weather events is still under the process of understanding as the physics behind its main cause is yet to be well understood (Schwenn *et al.* 2005). Geomagnetic storms are the outcomes due to the interaction of transferred solar wind energy towards the Earth's magnetosphere through magnetic reconnection. They come into existence as coronal mass ejections (CMEs) from Sun (Gopalswamy *et al.* 2007) and the corotating interaction regions (CIRs) which originates from the interaction of slow and fast

solar wind from coronal holes (Zhang *et al.* 2007). However, intense geomagnetic storms are mainly caused by CMEs (Gosling *et al.* 1990; Bothmer and Schwenn 1995; Tsurutani and Gonzalez 1998). The geomagnetic storms produce adverse effects (i) interrupt the communication and navigation system, (ii) affect the system of solar and Earth environment, (iii) cause threatfull power suspension and (iv) cause damage to satellited (Joselyn and McIntosh 1981; Gonzalez *et al.* 1994). Hence, there is a need of proper understanding of geomagnetic storms and their main causes.

Geomagnetic storms take place when there is long-lasting and large interplanetary magnetic field directed towards southward (Lindsay *et al.* 1995; Richardson *et al.* 2002, 2006; Gonzalez *et al.* 2004). Newton and Milson (1954) reported that largest geomagnetic storms occur in the span of years on either side of the peak phase of the solar cycles. Gupta Das and Basu (1965) inferred that outstanding events majorly occurs either in the ascending or descending phase of the solar cycle or in the both region leaving the peak region. In general, the geomagnetic storms are associated with CMEs and CIRs (Lei *et al.* 2007; Zhang *et al.* 2007). CMEs occur mostly when there is maximum sunspot number along

Table 1. List of all geomagnetic storms in the plunging time of Solar Cycle 24.

Year	Moderate storms (Dst = −50 nT to −100 nT)	Intense storms (Dst = −100 nT to −200 nT)	Severe storms (Dst< − 200 nT)	Total storms (in a year)
2015	52	2	2	56
2016	35	2	0	37
2017 (till 14/ 10/2017)	18	2	0	20
Total (in category)	105	6	2	113

with the abnormal ejections from the sun (MacQueen *et al.* 1986; Hundhausen 1993). On the other hand, CIRs are the huge scales structures that occur in the declining phase of the solar cycle. CIRs are associated with the fast solar wind from coronal holes which takes place within the period of 27 days (Smith and Wolf 1976; Gosling *et al.* 1978, 1981; Crooker and Cliver 1994; Tsurutani *et al.* 1995). The interplanetary coronal mass ejections are diagnosed on the basis of various solar wind structures including magnetic cloud (Burlaga *et al.* 1982), ejections with nearby magnetic field structure (Burlaga *et al.* 2001), bidirectional electron fluxes (Gosling *et al.* 1987) and interplanetary shocks (Farris *et al.* 1992). During the initial phase of geomagnetic storm there is sudden increase in the density/speed which is due to the strong shock found ahead of fast coronal mass ejections (Willis 1964). Beside this, the co-rotating interaction regions originally from the coronal hole with open magnetic field structure, meets with the slow speed stream coming from streamer belt where sunspots, filaments and active regions are situated closed to magnetic structure (Smith and Wolf 1976; Gosling and Pizzo 1999; Singh *et al.* 2010).

In the present study the detection of CMEs has been performed on the basis of its images by a new method that can be done without any human involvement on a real time data of 24 h per day. This method is a software package called CACTus (computer aided CME tracking), which detects CMEs in the form of chronographic images. The human interpretation of CMEs is somewhat doubtful whether the detection will be stable over solar cycle or not. Also, big and structured event can be analyzed, but small and weak events are generally not detected (Robbrecht and Berghmans 2004). This method on experimental ground shows excellent result to measure start time, principle angle, angular width, velocity, etc. Robbrecht and Berghmans (2004) showed the success rate of 94% and also said that by this software there are certain unreported cases that affect the CMEs detection statistics and case studies. Berghmans *et al.* (2002) reported that CME detection by this software is much faster.

For the present analysis to find the causes responsible for the different geomagnetic storms, CMEs have been detected with the help of CACTus software during the period from January 2015 to September 2017, i.e. the plunging/declining phase of Solar Cycle 24. Further the methods have been employed as described by Singh *et al.* (2017). The analysis method along with data and result with discussion are stated in Sections 2 and 3 respectively, and conclusions in Section 4.

2. Data and methodology

For the present study, the most important parameter known as disturbed storm time index (Dst) has been used which indicates the hourly variation of the horizontal component of Earth's magnetic field. Ring current, tail current and magnetospheric current also shows their contribution to Dst index which depends on the interaction of character of the solar wind with Earth's magnetosphere (Zhang *et al.* 2007). It has been found that ring current leads to intense storms, super intense storms and tail current leads to moderate storms (Kalegaev *et al.* 2005). Depending on the Dst index, geomagnetic storms are classified as weak storm (Dst = −30 nT to −50 nT), moderate storm (Dst = −50 nT to −100 nT), intense storm (Dst = −100 nT to −200 nT) and severe storm (Dst < −200 nT) (Loewe and Prölss (1997). During the analysis period from January 2015 to October 2017, we observed 105 moderate storms, 6 intense storms and 2 severe storms for the declining phase of Solar Cycle 24. Year-wise classifications of all 113 geomagnetic storms which occurred during study period are presented in Table 1. We have selected all the 6 intense and 2 severe geomagnetic storms for the present study. Observed severe and intense geomagnetic storms along with their solar characteristics are presented in Tables 2 and 3 respectively. In the table from the left to right, the columns represent the distribution as storm day (Day), minimum Dst index, time (UT) CME number (CME), onset time (earliest lift off indication, t_0), duration of lift off (dt0) in hours, principal angle (pa)

Table 2. List of Serve geomagnetic storms with Solar features ensued in the plunging time of Solar Cycle 24 (2015–2017).

Storm Day	Min Dst (nT)	Time (UT)	CME	t0	dt0	pa	da	v	dv	minv	maxv	Halo	Region	Location	Flare	Shock arrival date/time	ICME speed km/sec	TTI	TTC	TTS
17 March 2015	−222	23:00	78	15/03/2015 02:36	3	356	270	710	316	190	1736	III	2297	S17W25	C9.1	17 March 04:00 UT	609	50h	68h	68h
23 June 2015	−204	05:00	78	19/06/2015 06:42	8	151	128	364	134	165	670	II	2371	N12 E39	C8.1	22 June 18:00 UT	742	78h	56h	94h
			90	21/06/2015 02:36	2	13	116	976	301	428	1562	II	2367	S20W49	M2.6	22 June 18:00 UT	742	39h	56h	51h

counterclockwise from north in degree, angular width (da) in deg., median velocity (v) in km/s, variation (1 sigma) of velocity over the width of the CME (dv), lowest velocity detected within the CME (minv), highest velocity detected within the CME (maxv), halo which is categorized as II if da > 90°, III if da > 180°, IV if da > 270°, indicating potential halo/partial halo CME. In addition to this the solar parameters, viz. source region, location, flare type, ICME arrival time at the spacecraft and its speed (km/s), transit time observed from the solar CME appearance above the occulting disk to ICME arrival at the spacecraft (TTI), calculated maximum transit time (TTC) based on maximum solar wind speed and transit time observed from solar CME appearance above the occulting disk to storm Dst peak time (TTS) in hours are also presented. The resultant solar wind plasma and field parameters with 1h time resolution were obtained from the OMNI website at http://omniweb.gsfc.nasa.gov. The OMNI database is created using measurements from Wind, ACE, IMP-8. Hourly Dst value in the OMNI database is acquired from the website http://swdc.kugi.kyoto-u.ac.jp/dstdir.

To detect the cause of the selected geomagnetic storms the CACTus software data has been used. CACTus automatically detects CMEs in image sequence from the LASCO. Its output is similar to classic catalog which are faster and very important as per the space weather requirement (http://sidc.oma.be/cactus/catalog.php). It gives the information as an image and gives short description of every input. Webb *et al.* (2000) reported that CMEs that are Earth directed has stronger impact on Earth's magnetosphere that aids to explain the geomagnetic storm. Webb *et al.* (2000) and Cane *et al.* (2000) considered CMEs as halo with the angular width as 140° to 120° respectively. Singh *et al.* (2017) had taken CMEs as full halo CMEs with angular width of 360° and partial halo CMEs with the angular width as 160°. For the present study, depending on angular width (da), we have taken the CMEs categorized as da > 90°(II), da > 180° (III), and if da > 270° (IV) which indicates the potential halo/partial halo CME.

To show the correlation of CMEs with geomagnetic storms, the time window method has been taken as discussed by (Brueckner *et al.* 1998; Webb *et al.* 2000; Gopalswamy *et al.* 2000; Cane *et al.* 2000). There are two transit times available, one from the Sun to the spacecraft in the near-Earth space and the other from the Sun to the peak time of geomagnetic storms. The chosen fixed 1–5 days window refers to the second transit time because we use the Dst peak time as the reference point. Secondly we have used the speed of ICME derived from plasma and magnetic field measurements on board

Table 3. List of Intense geomagnetic storms with Solar features ensued in the plunging time of Solar Cycle 24 (2015–2017).

Storm Day	Min Dst (nT)	Time (UT)	CME NO	t0 with date/time	dt0	pa	da	v	dv	minv
07/10/2015	−124	23:00	Coronal Hole	4 October	–	–	–	–	–	–
20/12/2015	−155	23:00	46	16/12/2015 09:24 UT	2	47	92	512	129	260
01/01/2016	−110	01:00	95	28/12/2015 12:00 UT	5	211	256	89	176	102
13/10/2016	−104	18:00	16	08/10/2016 12:00 UT	2	285	12	569	236	158
28/05/2017	−125	08:00	15	23/05/2017 05:36 UT	2	251	116	192	39	121
08/09/2017	−142	02:00	04	04/09/2017 19:12 UT	4	333	288	624	564	221
			17	06/09/2017 12:12 UT	4	1	360	978	530	376

Storm Day	maxv	Halo	Region	Location	Flare	ICME arrival date/ time (UT)	ICME speed (km/sec)	TTI	TTC	TTS
07/10/2015	–	–	–	–	–	–	–	–	–	–
20/12/2015	657	II	2468	S15W02	C6.6	19 Dec. 16:00 UT	497	79 h	83 h	110 h
01/01/2016	977	III	2473	S22W05	C8.0	31 Dec. 01:00 UT	485	63 h	85 h	87 h
13/10/2016	804	NIL	2599	S14W49	C1.3	12 October 22:00 UT	426	84 h	97 h	128 h
28/05/2017	262	II	2660	S11W15	B4.4	27 May 15:00 UT	400	106 h	104 h	122 h
08/09/2017	1953	IV	2673	S10W02	M1.7	07 Sept. 23:00 UT	821	52 h	50 h	79 h
	1955	IV	2673	S10W30	X9.3	07 Sept. 23:00 UT	821	36 h	50 h	38 h

NIL = No HALO (Partial or Potential).

Wind (Ogilvie *et al.* 1995; Lepping *et al.* 1995) and the Advanced Composition Explorer (ACE) to calculate a maximum transit time from the Sun to the near-Earth space. In this paper, we used the speed of the ICME front which is often a well-defined shock front. The calculated time is the maximum possible transit time for those CMEs that initially have a high speed at the Sun and maintain or decrease the speed in their course toward the Earth. With the use of both solar wind data and solar flare associated CME, the final result has been discussed.

3. Results and discussion

The occurrence of 113 geomagnetic storms (105 moderate storms, 6 intense storms and 2 severe storms) with their Dst indices during the study period is shown in Table 1. Since weak and moderate geomagnetic storms have little or no significant effect on ionosphere and magnetosphere they are not discussed in detail. A detailed study has been carried out for the 6 intense and 2 severe storms. The details about different solar and geomagnetic parameters as well as the source identification of each severe and intense geomagnetic storm are given in Table 2 and Table 3 respectively. Table 1 shows that there are 52 moderate storms occurred in 2015, 35 in 2016 and up to September 2017 comparatively less number of about 18 moderate storms have occurred. Table 3 reflects that there are 2 intense storms during 2015 whereas during 2016 there are only 2 intense storms and there is the occurrence of 2 intense storms up to September 2017 also. For the severe storms analysis, it has been observed that only 2 severe storms had occurred during the year 2015 and nil during 2016 and 2017. This trend of storms has been reported for the declining phase of Solar Cycle 24. Recently Singh *et al.* (2017) reported that solar activity increases from 2008 to 2013 and suddenly decreases in 2014. In continuation to the decreasing trend of the solar activities observed, it can be inferred on the basis of work done earlier that it has been continued till September 2017.

As per the CMEs observed from CACTus software for the occurred geomagnetic storms, it has been observed that total 6 CMEs have been found for the intense storms in which 2 CMEs are categorized as category II (da > 90°), 1 CME is with the category III (da > 180°), 2 CMEs are of category IV (da > 270°) and 1 CME is not halo and 1 event is without CME. For the severe storms, 3 CMEs, in total has been obtained, one of category III in March 2015 and other 2 of category II in June 2015. Analysis shows that, all the total 9 CME associated events originated from active regions of the Sun in which the sources of 4 events were located in the western hemisphere and only one events have their source origin in the eastern hemisphere. The source origins of 4 events were close to the central meridian. It is observed that high-speed solar CMEs associated with intense as well as severe storms, decelerate during its course from the Sun to the Earth. Most of the observed transit times (TTC) for CMEs from the Sun to the near-Earth space are greater than the transit times from the Sun to the near-Earth space (TTI) and TTS (from the Sun to the Dst peak value) for both the intense as well as severe storms. Further in-depth analysis for the identification of different causes responsible for severe and intense geomagnetic storms, 2 different typical cases of severe storm and one typical case of intense storm are discussed below:

3.1 *Case studies*

3.1.1 Severe storm of March 17 2015 (Dst = −222 nT)
The severe storm event on March 17 2015 at 23:00 UT with Dst index as −222 nT seems to be associated with a halo CME on 15 March (02:36 UT) of category III, when the fixed 120 h time window is considered. The CME was originated from active region NOAA 2297 with maximum speed 1736 km/s and minimum 190 km/s and associated with GOES C1.4 flare (01:15 UT) at S17W25. To find out the cause behind the storm, we have used the solar wind density and speed, interplanetary magnetic field (B), the horizontal component of interplanetary magnetic field Bz, along with Dst plotted for a span of 5 days (15–20 March) as shown in Figure 1. From the figure it is noted that, as the shock arrived on interplanetary space at 04:00 UT on March 17, all parameters mentioned above jumped up. Total magnetic field B becomes 31.5 nT from 9.7 nT, speed raised to 609 km/s from 410 km/s and density $38.5/cm^3$ from $15.9/cm^3$. At that time Bz turned southward and remained southward for a longer time (about 23 hrs) having maximum value of -17.3 nT at 21:00 UT on 17 March resulting the server storm at 22:00 UT on the same day. Using ICME speed (speed of shock front) 609 km/s from graph the maximum transit time (TTC) from the sun to the near-Earth space is found to be 68 h. Observed transit time (TTI) for the CME to reach from Sun to Earth is 50 h which matches and is within the limit of maximum time. Thus severe storm event of 17 March 2015 may probably be caused by halo CME occurred on 15 March 2015.
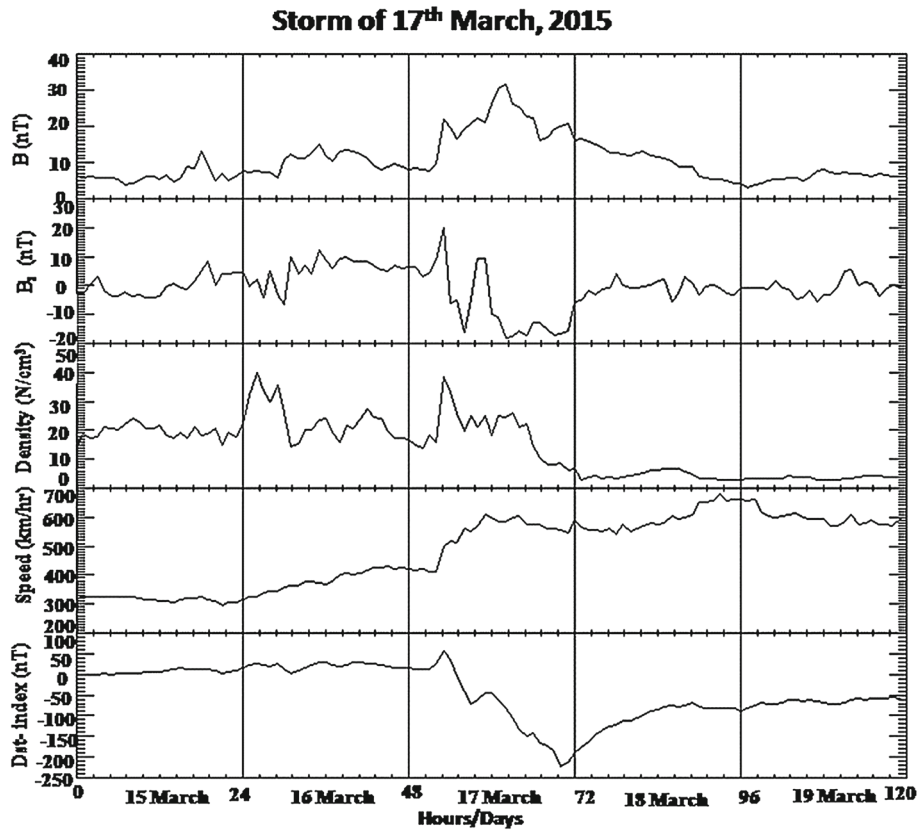
Storm of 17th March, 2015

Figure 1. Variations of solar wind parameters such as wind speed, density and IMF B, Bz and along with Dst index for a period of 5 days (from 15 March to 19 March 2015) for intense (17 March 2015 at 22 UT), severe storm (17 March 2015 at 23 UT) (with support from OMNI web plots https://omniweb.gsfc.nasa.gov/form/dx1.html).

3.1.2 Severe storm of June 23 2015 (Dst = −204 nT)
There are two consecutive geomagnetic storms of different class occurred on 22–23 June 2015. First is moderate (Dst = −51 nT), which occurred on 22 June at 16:00 UT. Second storm is serve class (Dst = −204 nT) observed at 04:00 UT on 23 June 2015. Within the 120 h fixed window, first storm has a halo CME candidate of category IV, occurred on 18 June at (17:24 UT), with maximum speed of 1024 km/s from active region AR 2371 and is associated with GOES M3.0 flare (17:36 UT) occurred at N12E39. This CME hit Earth atmosphere at 05:00 UT on 22 June. At that time speed raised to 446 km/s from 360 km/sec, density 26.9/cm^3 from 11.4/cm^3 and Bz oscillate between north and south became −8.3 nT from −2.1 nT, resulting a moderate storm. The Severe storm on 23 June has two candidate front side halo CMEs within the fixed 120 h window. First CME occurred on 19 June (06:42 UT) was originated from active region AR 2371 with maximum speed 670 km/sec and is associated with GOES C8.1 flare from N13E27, while second CME originated from AR 2367 with maximum speed of 1562 km/s on 21 June (02:36 UT) and is associated with GOES M2.6 flare S20W49

and followed by first CME. Both CMEs combined in space and hit Earth atmosphere at the same time (18:00 UT on 22 June). Figure 2 shows that, after the passage of shock (18:00 UT on 22 June) all parameters jumped up. Total magnetic field became 37.7 nT from 15.8 nT, solar wind speed and density jumped to 742 km/s from 515 km/s, and 49.9/cm^3 from 24.4/cm^3 respectively. During that time IMF Bz intensified to become -26.3 nT from -6.9 nT and then oscillating between north and south resulting a serve storm on June 23 at 04:00 UT. Based on solar CMEs only, we are not able to judge which of the two CMEs is the true source of serve storm. To confirm it, we have taken ICME speed from Figure 2, to calculate the maximum transit time (TTC) from the Sun to the near-Earth space. It is found to be 56 h. The observed transit times (TTI) for the two CMEs from the Sun to the Earth space are 78 h and 39 h. Hence serve storm on 23 June may probably be caused by 21 June CME, because transit time for first CME is out of limit of 56 h.

3.1.3 Intense storm of September 8 2017 (Dst = −142 nT) The Intense storm event occurred on
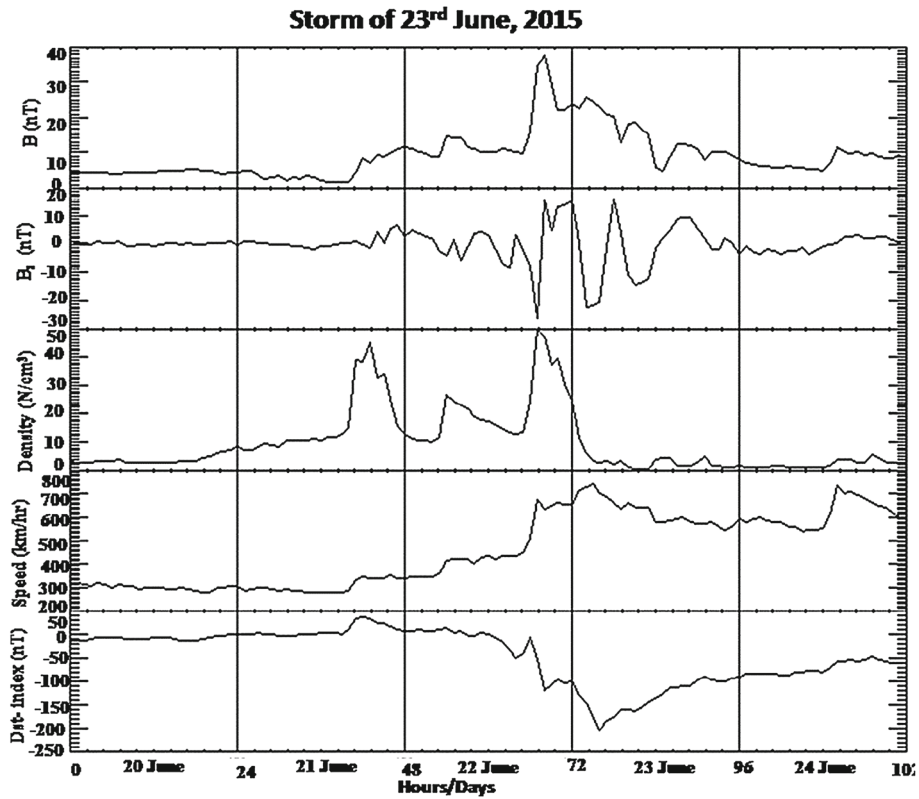
Figure 2. Variations of solar wind parameters such as wind speed, density and IMF B, Bz and along with Dst index for a period of 5 days (from 20 June to 24 June 2015) for intense (22 June 2015 at 21 UT, 23 June 2015 at 4 UT), severe storm on (23 June 2015 at 5 UT) (with support from OMNI web plots https://omniweb.gsfc.nasa.gov/form/dx1.html).

September 8 2017 at 01:00 UT with Dst index as -142 nT also has two halo CMEs candidates. First CME is associated with GOES M5.5 flare occurred on 4 September (19:15 UT) at S10W02, while second associated with GOES X9.3 flare observed on 6 September (12:12 UT) at S10W30. Both CMEs were originated from same active region AR2673. To find out the cause behind the storm, we have used the solar wind density, speed, magnetic field (B) and Bz, along with Dst plotted for a span of 5 days (6–10 September) as shown in Figure 3. As shock arrived at 22:00 UT on September 7, total magnetic field jumped from 10.5 nT to 27.3 nT and speed raised to 821 km/sec from 473 km/s but there are no significant changes in density. At that time IMF Bz which already pointed south ward became -23.6 nT from -8.1 nT and has remained southward resulting minimum Dst value to -142 nT. With the help of ICME speed (821 km/sec) the calculated transit time (TTC) is to be found 50 h, whereas observed transit times (TTI) for these CMEs are to be found 52 hrs and 34 h. Thus intense storm event of 8 September 2017 may be result of impact of both the CMEs.

All selected severe storms and intense storms are associated with the southward interplanetary magnetic field, indicating that the magnetic reconnection is the main mechanism for solar wind energy transfer to the magnetosphere (Gonzalez *et al.* 2004). Previous studied of the intense geomagnetic storms and their interplanetary origins (Tsurutani *et al.* 1995; Tsurutani and Gonzalez 1998; Gonzalez *et al.* 2004; Zhang *et al.* 2007; Singh *et al.* 2017) reported that about 80% of the intense storms which occurred in ascending phase of solar cycle were associated with ICMEs whereas CIRs caused only 13% of the intense storms. Our results show that out of 6, 5 events are caused by the ICMEs and only one event is caused by CIR. Bothmer and Schwenn (1995) also found that 42 (98%) out of 43 events that occurred during 1966 to 1990 were caused by ICMEs and one was caused by a CIR. Comparing present results with those of Bothmer and Schwenn (1995) and Zhang *et al.* (2007) it is noted that the role of CIR in inducing intense geomagnetic storms remains unaltered even during weak solar cycle. Subramanian and Dere (2001) reported that 9 (82%), out of 11 CMEs driven intense storms were associated with active regions whereas 5 (19%) moderate and 2 (18%) intense storms were not associated with active regions. The latter ones may be associated with quite-sun regions. The difference in our results with other reported results may be attributed to the fact that the present study period is in descending
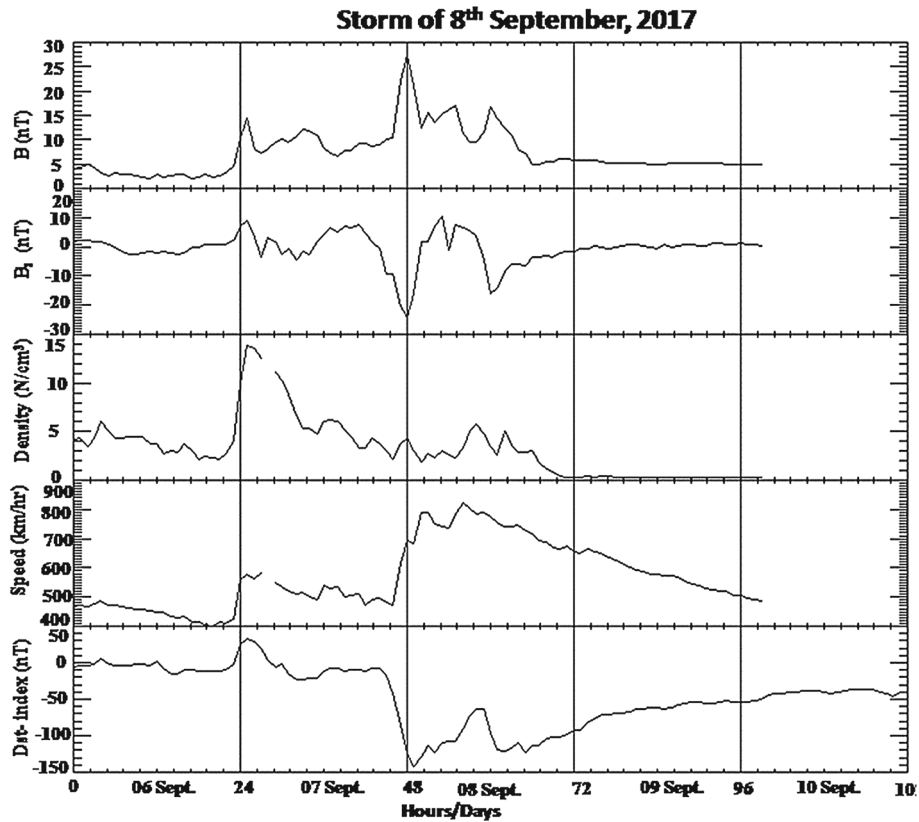
Figure 3. Variations of solar wind parameters such as wind speed, density and IMF B, Bz and along with Dst index for a period of 5 days (from 06 Sept. **to** 10 Sept. 2017) for intense (08 September 2077 at 2 UT) (with support from OMNI web plots https://omniweb.gsfc.nasa.gov/form/dx1.html).

phase of weak solar cycle. In the study period of storms only 105 moderate, 6 intense and only 2 severe storms are observed. This shows the weakness of geomagnetic storms in Solar Cycle 24. Kilpua *et al.* (2014) have studied the cause of weakness of Solar Cycle 24 and concluded that it was due to the weak southward IMF and lack of strong ICME which led to in particular weak ring current response and the solar wind magnetosphere coupling efficiency.

4. Summary and conclusion

On the basis of the CACTus software analysis the occurrence of total 113 geomagnetic storms during declining phase of Solar Cycle 24 (2015–2017) out of which 6 intense storms and 2 severe storms has been analysed in detail. In the fixed time window the likely sources such as CME, CIR, etc were searched. In the adoptive time window the possible CME/CIR or their combinations are pin-pointed.

It has been found that mostly the CMEs (except one event with CIR) are responsible for the intense and severe storms occurred during 2015–2017. It is further observed that the CMEs are mostly partial with angular

width ranging from 100° to 270° and only two CMEs are full CMEs which are responsible for the intense storms during 2015–2017. The severe storm event of 17 March 2015 may be caused by a halo CME occurred on 15 March 2015. The severe storm on 23 June 2015 may be caused by 21 June 2015 halo CME. The intense storm event occurred on September 8 2017 at 01:00 UT with Dst index as -142 nT has two halo CMEs candidates and after calculated transit time (TTC) with the help of ICME speed, it is observed that intense storm event of September 8 2017 may be result of impact of both the CMEs. Thus all analyzed intense geomagnetic storms are due to coronal mass ejection at the Sun except one event which is related to CIR. Therefore, we can conclude that ICMEs are the main source for major geomagnetic storms and a CIR is only occasionally the source of intense or severe geomagnetic storm event. Most of our above results are in good accordance with other reported results.

Acknowledgements

References

Berghmans D., Foing B. H., Fleck B. 2002, Symposium. ESA SP., 508, 437

Bothmer V., Schwenn R. 1995, J. Geomagn. Geoelectr., 47, 1127

Brueckner G. E., Delaboudiniere J. P., Howard R. A., Howard R. A., Paswaters S. E., St, Cyr O. C., Schwenn R., Lamy P., Simnett G. M., Thompson B., Wang D. 1998, Geophys. Res. Lett., 25, 3019

Burlaga L. F., Klein L., Sheeley N. R., Michels D. J, Howard R. A., Koomen M. J., Schwenn R., Rosenbauer H. 1982, Geophys. Res. Lett., 9, 1317

Burlaga L. F., Skoug R. M., Smith C. W., Webb D. F., Zurbuchen T. H., Reinard A. 2001, J. Geophys. Res. Sp. Phys., 106, 20957

Cane H. V., Richardson I. G., St. Cyr O C. 2000, Geophys. Res. Lett., 27(21), 3591

Crooker N. U, Cliver E. W. 1994, J. Geophys. Res., 99, 23383

Farris M. H., Russell C. T., Thomsen M. F., Gosling J. T. 1992, J. Geophys. Res., 97, 19121

Gonzalez W. D., DalLago A. C., Gonzalez A. L., Vieira L. E. A., Tsurutani B. T. 2004, J. Atmos. Solar- Terr. Phys., 66, 161

Gonzalez W. D., Joselyn J. A., Kamide Y., Kroehl H. W., Rostoker G., Tsurutani B. T., Vasyliunas V. M. 1994, J. Geophys. Res., 99(A4), 5771

Gopalswamy N., Yashiro S., Akiyama S. 2007, J. Geophys. Res., 112, A06112, 1

Gopalswamy N., Lara A., Lepping R. P., Kaiser M. L., Berdichevsky D., St. Cyr O. C. 2000, Geophys. Res. Lett., 27, 145

Gosling J. T., Asbridge J. R., Bame S. J., Feldman W. C. 1978, J. Geophys. Res., 83, 14001

Gosling J. T., Baker D. N., Bame S. J. 1987, J. Geophys. Re., 92, 8519

Gosling J. T., Borrini G, Asbridge J. R., Bame S. J., Feldman W. C., Hansen R. T. 1981, J. Geophys. Res., 86, 5438

Gosling J. T., Bame, S. J., McComas D. J., Phillips J. L. 1990, Geophys. Res. Lett., 17, 901

Gosling J. T., Pizzo V. J. 1999, Space Sci. Rev., 7, 21

Gupta Das M. K., Basu D. 1965, Nature 208, 739

Hundhausen, A. J. 1993, J. Geophys. Res., 98, 13177

Joselyn J. A., McIntosh P. S. 1981, J. Geophys. Res., 86, 4555

Kalegaev V., Ganushkina N., Pulkkinen T., Kubyshkina M. V., Singer H. J., Russell C. T. 2005, Ann. Geophys., 23, 523

Kilpua E. K. J., Luhmann J. G., Jian L. K., *et al.* 2014, J. Atmos. Solar-Terrestr. Phys., 107, 12. https://doi.org/10.1016/j.jastp.2013.11.001

Lei J., Syndergaard S., Burns A. G. 2007, J. Geophys. Res. Sp. Phys., 112, 1

Lepping R. P., Acũna M. H., Burlaga L. F. 1995, Space. Sci. Rev., 71, 207

Lindsay G. M., Russel C. T., Luhmann J. G. 1995, J. Geophys. Res., 100, 16999

Loewe C. A., Prölss G. W. 1997, J. Geophys. Res., 102, 14209

MacQueen R. M., Hundhausen A. J., Conover C. W. 1986, J. Geophys. Res., 91, 31

Newton H. W., Milson A. S. 1954, J. Geophys. Res. Atmos., 59(2), 203

Ogilvie K. W., Chornay D. J., Fritzenreiter R. J. 1995, Space. Sci. Rev., 71, 55

Richardson T. J., Paularena D., Wang K. I. C., Burlaga L. F. 2002, J. Geophys. Res., 107(A4) 1041, 1

Richardson J. D., Liu Y., Wang C., Burlaga L. F. 2006, Adv. Space Res., 38, 528

Robbrecht E., Berghmans D. 2004, Astron. Astrophys., 425, 1097

Schwenn R., Dal Lago A., Huttunen E., Gonzalez W. D. 2005, Ann. Geophys., 23, 1033

Singh A., Rathore V. S., Singh R. P., Singh A. K. 2017, Adv. Space. Res., 59(5), 1209

Singh A. K., Siingh D., Singh R. P. 2010, Surv. Geophys., 31, 581

Siscoe G., Schwenn R. 2006, Space Sci. Rev., 123(1), 453

Smith E. J., Wolf, J. H. 1976, Geo-phys. Res. Lett., 3, 137

Subramanian P., Dere K. P. 2001, Astrophys J., 561, 372. https://doi.org/10.1086/323213

Tsurutani B. T., Gonzalez W. D., Gonzalez A. L. C., Tang F., Arballo J. K., Okada M. 1995, J. Geophys. Res. Sp. Phys. 100, 21717

Tsurutani, B. T, Gonzalez W. D. 1998, Geophys. Mono. Ser., 98, 77

Webb D. F., Cliver E. W., Crooker N. U., StCyr O. C., Thompson B. J. 2000, J. Geophys. Res., 105, 7491

Willis D. M. 1964, J. Atmos. Terr. Phys., 26, 581

Zhang J., Richardson I. G., Webb D. F., Gopalswamy N., Huttunen E., Kasper J. C., Nitta N. V., Poomvises W., Thompson B. J., Wu C. -C., Yashiro S., Zhukov A. N. 2007, J. Geophys. Res., 112, A10102, 1